Applied Soft Computing Journal 89 (2020) 106145

Contents lists available at ScienceDirect

Applied Soft Computing Journal

journal homepage: www.elsevier.com/locate/asoc

Tensor alternating least squares grey model and its application to short-term traffic flows

Huiming Duan [a,b,*], Xinping Xiao [b], Jie Long [a], Yongzhi Liu [a]

[a] School of Science, Chongqing University of Posts and Telecommunications, Chongqing, 400065, China
[b] School of Science, Wuhan University of Technology, Wuhan, 430070, China

ARTICLE INFO

Article history:
Received 23 September 2019
Received in revised form 3 January 2020
Accepted 27 January 2020
Available online 31 January 2020

Keywords:
Multi-mode traffic flow data
Tensor Tucker decomposition
Alternating least squares
GM (1,1) model

ABSTRACT

Traffic flow data, as an important data source for the research and development of intelligent transportation systems, contain abundant multi-mode features. In this paper, a high-dimensional multi-mode tensor is used to represent traffic flow data. The Tucker tensor decomposition least squares algorithm is used to establish the tensor alternating least squares GM (1,1) model by combining the modelling mechanism of the grey classical model GM (1,1) with the algorithm, and the modelling steps are obtained. To demonstrate the effectiveness of the new model, first, the multi-mode traffic flow data are represented by the tensor model, and the correlation of the traffic flow data is analysed. Second, two short-term traffic flow prediction cases are analysed, and the results show that the performance of the GM (1, 1) model based on the tensor alternating least squares algorithm is obviously better than that of the other models. Finally, the original tensor data and the approximate tensor data during the peak period from 8:00 to 8:30 a.m. for six consecutive Mondays are selected as the experimental data, and the effect of the new model is much better than that of the GM (1,1) model of the original tensor data.

1. Introduction

Intelligent transportation systems (ITS) are a type of traffic control information management system that has been developed in recent years. Short-term traffic flow forecasting is an important part of ITS. Improving short-term traffic flow forecasting precision can provide support for intelligent transportation systems. Traffic flow data, as an important data source for the research and development of ITS, contain abundant multi-mode features. Tensors are generalizations of vector and matrix models that can represent multi-dimensional data and have multi-mode characteristics. At the same time, traffic data are observed from different modes of week, day, space and time, showing significant multi-mode features and strong multi-correlation [1,2]. The use of tensors to represent multi-dimensional data with multi-modal features [3] can overcome the shortcomings of vector and matrix data forms that have difficulty characterizing multi-dimensional features [4]. Therefore, to improve the accuracy of short-term traffic flow predictions, the multi-mode characteristics of traffic data and the overall trends of traffic flow data can be fully considered to improve the accuracy of short-term traffic flow predictions.

With the rapid development of ITS, researchers have performed extensive research on traffic flow predictions. Pattern information is often divided into the vector data stream form, matrix data stream form and tensor data stream form as research objects for short-term traffic flow predictions. Short-term traffic flow predictions more commonly use vector data flow than other forms: Stephanedes [5] used a historical average model and the autoregressive integral moving average (ARIMA) model [6] to predict short-term traffic flow. Nonlinear prediction methods, support vector regression (SVR) models [7] and support vector machine theory [8] have been used to mine the nonlinear characteristics of traffic data. Subsequently, spectral analysis [9] prediction models, chaos prediction models [10], neural networks [11] and other model types have exhibited improved prediction effects on high-quality historical sample databases.

Short-term traffic flow predictions in the form of matrix data flow: multivariate time series prediction models regard the traffic data from different spatial points as interrelated variables and construct the traffic data as multivariate time series [12]. Multi-section short-term traffic flow predictions are mainly based on the traffic flow data from multiple sections of the road. Based on a time series of traffic data, Cheng et al. [13] reconstructed daily and weekly time series of traffic data to predict the short-term traffic flow. Guo et al. [14] used the Kalman filter to predict the seasonal autoregressive real-time traffic flow. Zhang et al. [15] analysed the periodic trend, certainty and volatility of

* Corresponding author at: School of Science, Chongqing University of Posts and Telecommunications, Chongqing, 400065, China.
E-mail address: huimingduan@163.com (H.M. Duan).

https://doi.org/10.1016/j.asoc.2020.106145
1568-4946/

traffic data using spectral analysis technology, ARIMA and the generalized autoregressive conditional heteroskedastic (GARCH) model. Hong [16] proposed a seasonal SVR prediction model. Yang et al. [17] created a coupled prediction of time series data and cross-section data at intersections, and these methods achieved good results.

Short-term traffic flow predictions in the form of tensor data flow: traffic data are observed from different modes of the week, day, space and time, and the traffic data show significant multi-mode features. To improve the accuracy of short-term traffic flow predictions, the multi-mode characteristics of traffic data are fully considered. For example, Tan et al. [18] reconstructed the daily time series and weekly time series of traffic data to predict the short-term traffic flow based on the time series of traffic data. Tan et al. [19] expressed traffic flow data with a tensor model and proposed a new method for filling data with a dynamic tensor. Duan et al. [20,21] used the multi-mode characteristics of traffic flow data to expand the traffic flow data by using the "week-day-time" mode and establish a coupled tensor multi-mode model and the grey prediction model for tensor dynamics, and this method achieved better results than previous methods.

The above prediction models are usually based on large sample sizes and cannot be used to solve small-scale problems. At the same time, short-term traffic flow forecasting uses road traffic flow state data that are dynamically acquired to infer data on the future traffic flow state. The time scale of the traffic flow data is generally limited to 15 min. The traffic flow data in the previous period obviously have the greatest impact on the next period if one hour is taken as the time scale. The interval between records is 5 min; thus, only 12 groups of data are collected in one hour. Due to the daily time scales, traffic flow data are composed of small sample sizes. In addition, there are uncertain factors in the traffic system, such as vehicle characteristics, weather factors and the abnormal loss of traffic flow data. The traffic flow is an integral value that can approximately determine the range of true or abnormal data according to the traffic conditions and measured values in the front and back periods, and its range is a discrete set. These uncertainties within a certain interval or a set of numbers reflect the characteristics of the grey system. Simultaneously, the grey prediction model has strong adaptability and can adequately handle mutation parameters.

The grey prediction model [22] is an important part of grey theory. After more than 30 years of development, this model has been widely used in agriculture, industry, society, economics, transportation, energy, medicine and other fields [23–31]. With much research, the classic grey prediction model, the GM (1,1) model, has been extended to different types of models, such as GM (1, N) [32], DGM (1, 1) [33], NDGM (1,1) [34,35], ONGM (1,1) [36], ENGM (1,1) [37] and other new prediction models. At the same time, GM (1,1) [38–45] has been studied from multiple perspectives such as data accumulation, optimization of background values, model properties, and modelling mechanisms, which has promoted the development and perfection of the theoretical system of the grey prediction model. Short-term traffic flow prediction is an important application of the grey model [17,20,21,34–39]. Hsu et al. [46] proposed an adaptive GM (1,1) model for traffic prediction of an intersection without a detector. Guo et al. [47] established a grey nonlinear delay GM (1,1) model for short-term traffic flow. Bezuglov and Comert [48] established a GM (1,1) model and a grey Verhulst model with Fourier error correction, which achieved good prediction results in the prediction of short-term traffic flow speed and travel time. Xiao et al. [49] proposed a seasonal GM (1,1) rolling prediction model based on the cycle truncation accumulated generating operation (CTAGO). According to the law of vehicle conservation, Xiao et al. [50] established a new dynamic grey prediction model to predict the short-term traffic flow. Lu et al. [51] used the nonlinear grey Bernoulli equation to obtain the grey prediction model for traffic flow prediction and achieved good results. According to the mechanical characteristics of traffic flow data, Duan et al. [52] applied the grey inertia model to predict short-term traffic flow and determine the traffic flow state.

Table 1
Abbreviations and corresponding definitions for the different grey prediction models.

Number	Abbreviation	Definition
1.	GM (1,1)	Grey model with one variable and one first order equation
2.	ENGM (1,1)	Exact nonhomogeneous grey model
3.	ONGM (1,1)	Optimized NGM(1,1,k,c) model
4.	Verhulst	Verhulst grey model
5.	ARIMA	Autoregressive integrated moving average model
6.	ANN	Artificial neural network
7.	TALSGM (1,1)	Tensor alternating least squares grey model

However, the abovementioned short-term traffic flow prediction methods (vector data flow, matrix data flow, tensor flow data flow), as well as the following grey prediction methods, care about only the nonlinearity, volatility, periodicity and other characteristics of a single time series change or spatial change at the target road section. These methods fail to make full use of the multi-mode characteristics of traffic flow data to deeply determine the temporal correlation of traffic flow data, especially the "weekday time" traffic flow data characteristics, which to some extent affect the prediction. At the same time, the above models directly usually use the collected traffic flow data in the model. These models do not make full use of the multi-mode characteristics of traffic flow and fail to grasp the overall trends of traffic flow, which also affects the prediction by the model.

Therefore, to better mine the multiple pattern characteristics of traffic data, such as weeks, days and hours, this paper uses tensors to represent the multi-pattern characteristics of traffic flow data and uses the tensor alternating least squares method to fully mine the traffic data. Combined with the modelling mechanism of the classic GM (1,1) model, a grey prediction model of tensor traffic multiplication is proposed. This paper discusses the tensor representation of traffic flow data in the minute, hour, day and week modes and analyses the correlation of the data. At the same time, cases are given to analyse the validity of the GM (1,1) model for tensor alternating multiplication.

In the full text, the different abbreviations are for the different grey prediction models. Abbreviations and their meanings are provided in Table 1.

The remaining chapters of this paper are arranged as follows. Part 2 introduces the basis of tensor algebra and the theory of the tensor Tucker decomposition model. The third part establishes the tensor alternating least squares grey forecasting model, and the fourth part describes a case study and provides a comparative discussion. Part 5 presents the conclusion.

2. Tensor model foundations

This section introduces the definitions, basic operations and related properties of tensors.

2.1. Tensor algebraic basis

The first-order tensor is a vector, the second-order tensor is a matrix, and the third-order and higher-order tensors are called higher-order tensors (high-dimensional tensors).

Definition 2.1 ([4]). Mode-K fibre bundle: Fix all indexes other than the K index in the n-order tensor to obtain a vector, which is called the Mode-K fibre bundle.

Through the above definition, the column vector of the matrix is the mode-1 fibre bundle, and the row vector of the matrix is the mode-2 fibre bundle. The mode-1 fibre bundle of the third-order tensor is called the column fibre, the mode-2 fibre is called the row fibre, and the mode-3 fibre is called the tube fibre. The three fibres are written as $x_{:,j,k}$, $x_{i,:,k}$, and $x_{i,j,:}$, as shown in Fig. 1.

Definition 2.2 ([15]). Tangent: Fix all indexes except two indexes in the n-order tensor to obtain a matrix, which is called a tangent.

For the third-order tensor, there are three kinds of tangents. The tangent plane of the third-order tensor is shown in Fig. 2. The tangent matrix of the third-order tensor is expressed in the form of $X_{:,:,k}$, the lateral tangent is expressed in the form of $X_{:,j,:}$, and the horizontal tangent is expressed in the form of $X_{i,:,:}$.

Definition 2.3 ([15]). Mode-N expansion: The mode-n expansion of a tensor is also called the matrix of a tensor. The mode-n expansion is to quantify the tensor as a matrix and to make a different matrix according to the direction of the mode-n fibres. The matrix of mode-n expansion is $X_{(n)}$.

Definition 2.4 ([4]). Set two N-order tensors as $\chi_1 \in R^{I_1 \times I_2 \times \cdots \times I_N}$ and $\chi_2 \in R^{I_1 \times I_2 \times \cdots \times I_N}$, then

$$\langle \chi_1, \chi_2 \rangle = \sum_{i_1=1}^{I_1} \sum_{i_2=2}^{I_2} \cdots \sum_{i_N=1}^{I_N} x_{i_1 i_2 \cdots i_N} y_{i_1 i_2 \cdots i_N}$$

is the inner product of the two N-order tensors.

Definition 2.5 ([4]). Set the N-order tensor as $\chi \in R^{I_1 \times I_2 \times \cdots \times I_N}$ and define the Frobenius norm as follows:

$$\|\chi\|_F = \sum_{i_1=1}^{I_1} \sum_{i_2=2}^{I_2} \cdots \sum_{i_N=1}^{I_N} x_{i_1 i_2 \cdots i_N}^2$$

At the same time, the Frobenius norm is also called the modulus of the tensor.

Definition 2.6 ([4]). Let the N-order tensor be $\chi_1 \in R^{I_1 \times I_2 \times \cdots \times I_N}$ and M-order tensor be $\chi_2 = R^{I_1 \times I_2 \times \cdots \times I_N}$, define: $\chi_1 \otimes \chi_2 = x_{i_1 i_2 \cdots i_N} y_{i_1 i_2 \cdots i_M}$, as the product of the two tensors.

Definition 2.7 ([4]). If the N-order tensor $\chi \in R^{I_1 \times I_2 \times \cdots \times I_N}$ can be expressed in the form of N vector outer products, that is,

$$\chi = x_1 \otimes x_2 \otimes \cdots \otimes x_N, x_k \in R^{I_k} (k = 1, 2, \ldots, N)$$

tensor χ is called a tensor with rank 1.

2.2. Tensor Tucker decomposition

Tucker decomposition is also called higher-order singular value decomposition (HOSVD). Tucker decomposition is a special form of decomposition of a tensor into a core tensor and a factor matrix of the same dimension. Tensor data are composed of the corresponding factor matrix along each modular multiplication of the core tensor. Therefore, Tucker decomposition is also a high-order principal component analysis method.

Definition 2.8 ([4]). Tucker decomposition of third-order tensor: Set such a third-order tensor $\chi \in \mathbb{C}^{P \times Q \times R}$; its Tucker decomposition can be expressed as a mode of the product of a core tensor and a three-factor matrix; that is,

$$\chi = \sum_{l=1}^{L} \sum_{m=1}^{M} \sum_{n=1}^{N} \vartheta_{l,m,n} (u_l \circ v_m \circ w_n) = \vartheta \times_1 U \times_2 V \times_3 W \tag{2.1}$$

where "$\circ$" is called the outer product operator, $\vartheta \in \mathbb{C}^{L \times M \times N}$ is called the core tensor of this Tucker decomposition, and the Tucker decomposition of the χ tensor can also be expressed as $\chi = [\![\vartheta : U, V, W]\!]$. Each element in the core tensor reflects the relationship between the factor matrix U, V, W. Concurrently, the Tucker decomposition model is analysed from the element direction of the tensor, which can also be expressed as:

$$\chi_{p,q,r} = \sum_{l=1}^{L} \sum_{m=1}^{M} \sum_{n=1}^{N} \vartheta_{l,m,n} (u_{p,l} \circ v_{q,m} \circ w_{r,n}) \tag{2.2}$$

where L, M, N is the matrix rank of the third-order tensor χ under the expansion of mode-1, mode-2 and mode-3.

By analysing the Tucker decomposition model from the tangent form of the tensor, three corresponding representations can be obtained. If the left and right-side sections of the third-order tensor χ are made, then equation (2.2) can change into:

$$X_{:,q,:} = W \sum_{j=1}^{J} v_{q,j} \circ G_{:,j,:} \circ U^T \quad q = 1, 2, \cdots, Q$$

Therefore, if the third-order tensor χ is quantized into a matrix form, Eq. (2.1) can be written as follows:

$$X_{(1)} = U G_{(1)} (W \otimes V)^T$$
$$X_{(2)} = V G_{(2)} (W \otimes U)^T$$
$$X_{(3)} = W G_{(3)} (V \otimes U)^T$$

where $G_{(1)}$, $G_{(2)}$, and $G_{(3)}$ represent the expansion matrices of the core tensor.

To convert the third-order tensor χ into a vector form, Eq. (2.1) can be written as follows:

$$vec(\chi) = (W \otimes V \otimes U) vec(\vartheta)$$

for tensor χ of order N, its Tucker decomposition model can be written as follows:

$$\chi = \vartheta \times_1 U^{(1)} \times_2 U^{(2)} \times_3 \cdots \times_N U^{(N)} \tag{2.3}$$

then the decomposition equation (2.3) has such a reversal transformation:

$$\vartheta = \chi \times_1(U^{(1)})^T \times_2 (U^{(2)})^T \times_3 \cdots \times_N (U^{(N)})^T \tag{2.4}$$

3. Establishing the tensor alternating least squares grey prediction model

This section describes and proposes the tensor alternating least squares (ALS) GM (1,1) model (TALSGM (1,1) model).

3.1. Calculation method of the Tucker tensor decomposition

ALS is a method for solving optimization problems. The ALS algorithm can obtain the optimal solution for a problem from a large amount of data and solve the Tucker tensor decomposition problem.

The Tucker decomposition of the third-order tensor $\chi \in \mathbb{C}^{P \times Q \times R}$ is discussed as an example.

$$\min_{\hat{\chi}} \|\chi - \hat{\chi}\|_F^2$$
$$\text{such that } \hat{\chi} = \sum_{l=1}^{L} \sum_{m=1}^{M} \sum_{n=1}^{N} \vartheta_{l,m,n} (u_l \circ v_m \circ w_n) \tag{3.1}$$

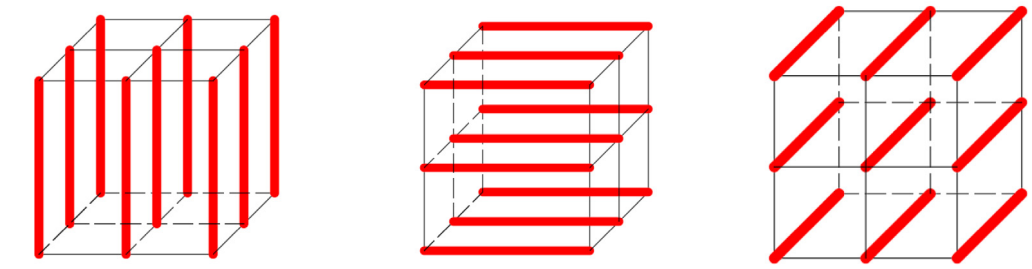

(a) Column fibres (b) Travelling fibres (c) Tubular fibres

Fig. 1. Three fibre bundles of the third-order tensor.

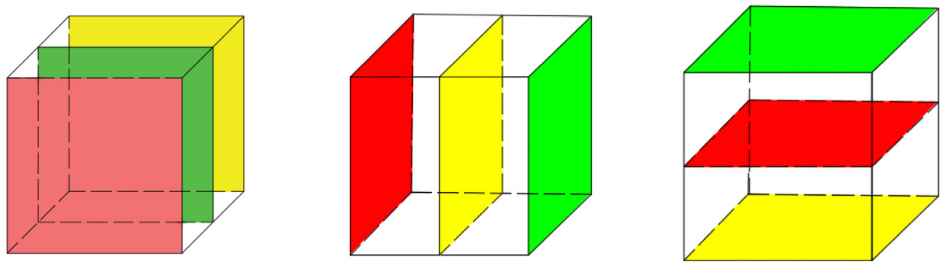

(a) Positive section (b) Side section (c) Horizontal section

Fig. 2. Three sectional diagrams of third-order tensors.

The solution steps for the ALS method of the Tucker decomposition for the tensor χ are given below.

Step 1. The known factor matrices V, W and the core tensor ϑ are used to obtain the factor matrix $\hat{U}$, and then $\hat{U}$ is updated to the factor matrix U. Then, Eq. (3.1) is equivalent to the following:

$$\min_{\hat{U}} \|X_{(1)} - UG_{(1)}(W \otimes V)^T\|_F^2 \tag{3.2}$$

Step 2. From Eq. (3.2), it is known that solving the Tucker decomposition problem becomes the least squares solution of the equation $X_{(1)} = UG_{(1)}(W \otimes V)^T$. By multiplying both sides of the equation by $W \otimes V$, the following equation can be obtained:

$$X_{(1)}(W \otimes V) = UG_{(1)}(W \otimes V)^T(W \otimes V) \tag{3.3}$$

Step 3. The singular value decomposition of Eq. (3.3) is obtained as follows:

$$X_{(1)}(W \otimes V) = E_1 \sum_1 F_1^T$$

In this case, the column vectors behind the L column of the singular value matrix E_1 are removed, and only the remaining column vectors are taken. Thus, the estimated value $\hat{U} = E_1(:, 1:L)$ is obtained, and let $U = \hat{U}$.

Step 4. Next, steps similar to the above three steps are performed, the matrix a is fixed, and the estimated value of the matrix V is determined, which is equivalent to the singular value decomposition of $X_{(2)}(W \otimes U)$:

$$X_{(2)}(W \otimes U) = E_2 \sum_2 F_2^T$$

Similarly, only column M in front of E_2 is selected to obtain the estimated value $\hat{V} = E_2(:, 1:M)$, and we then set $V = \hat{V}$. Then, the matrices U, V are fixed, the estimated value of matrix W is obtained, and the singular value decomposition of $X_{(3)}(V \otimes U)$ is performed.

$$X_{(3)}(V \otimes U) = E_3 \sum_3 F_3^T$$

The first N columns of the matrix E_3 are extracted to obtain the estimated value $\hat{W} = E_3(:, 1:N)$, and we then let $W = \hat{W}$.

Step 5. Use the three new factor matrices that are calculated by the above steps. Then, according to the inverse transformation of the tensor decomposition (3.3), the estimated value of the core tensor can be calculated as follows:

$$\hat{\vartheta} = \chi \times_1 \hat{U}^T \times_2 \hat{V}^T \times_3 \hat{W}^T$$

Step 6. Finally, according to Eq. (3.3), the core tensor estimates are multiplied by the three-factor matrix estimates, and then the approximate third-order tensor $\hat{\chi}$ is calculated. If $\hat{\chi}$ satisfies Eq. (3.1), the output factor matrix and the core tensor are obtained. If the condition is not satisfied, the first step is returned to continue the iteration.

The ALS algorithm for the third-order tensor Tucker decomposition is shown in Algorithm 1.

3.2. GM (1,1) model

This section mainly introduces the definition and properties of the GM (1,1) model as follows:

Let $X^{(0)}$ be the original data sequence:

$$X^{(0)} = (x^{(0)}(1), x^{(0)}(2), \ldots, x^{(0)}(n)), \tag{3.4}$$

$X^{(1)}$ is the first-order cumulative generating sequence of $X^{(0)}$.

$$X^{(1)} = (x^{(1)}(1), x^{(1)}(2), \ldots, x^{(1)}(n)), \tag{3.5}$$

where $x^{(1)}(k) = \sum_{i=1}^{k} x^{(0)}(i)$, $k = 1, 2, \ldots, n$.

$Z^{(1)}$ is the neighbouring mean generating sequence of $X^{(1)}$:

$$Z^{(1)} = (z^{(1)}(2), z^{(1)}(3), \ldots, z^{(1)}(n)) \tag{3.6}$$

where $z^{(1)}(k) = 0.5(x^{(1)}(k) + x^{(1)}(k-1))$, $k = 2, 3, \ldots, n$.

Definition 3.1. Let sequences $X^{(0)}$, $X^{(1)}$ and $Z^{(1)}$ be the same as (3.4)–(3.6), respectively, then call

$$x^{(0)}(k) + az^{(1)}(k) = b \tag{3.7}$$

Algorithm 1: The algorithm based on ALS to find the factor matrix

Input: The original third-order tensor $\chi \in \mathbb{C}^{P\times Q\times R}$,an error threshold ε

Ouput: The best factor matrix U,V,W,a core tensor ϑ

Set: The number of columns for factor matrices to L,M,N

Initialize the $U_1 \in \mathbb{C}^{P\times L}, V_1 \in \mathbb{C}^{Q\times M}, W_1 \in \mathbb{C}^{R\times N}, \delta \leftarrow \chi$

While $\| \delta \|_F \geq \varepsilon$

$A \leftarrow X_{(1)}(W_k \otimes V_k)$

$A{=}E_1 \sum_1 F_1^T$

$\hat{U}_{k+1} \leftarrow E_1(:,1:L)$

$B \leftarrow X_{(2)}(W_k \otimes U_{k+1})$

$B{=}E_2 \sum_2 F_2^T$

$\hat{V}_{k+1} \leftarrow E_2(:,1:M)$

$C \leftarrow X_{(3)}(V_{k+1} \otimes U_{k+1})$

$C{=}E_3 \sum_3 F_3^T$

$\hat{W}_{k+1} \leftarrow E_3(:,1:N)$

$\hat{\vartheta} \leftarrow \chi \times_1 \hat{U}_{k+1}^T \times_2 \hat{V}_{k+1}^T \times_3 \hat{W}_{k+1}^T$

$\delta \leftarrow \chi - \sum_{l=1}^{L}\sum_{m=1}^{M}\sum_{n=1}^{N} \vartheta_{l,m,n}(u_l^{(k+1)} \circ v_m^{(k+1)} \circ w_n^{(k+1)})$

end

$U \leftarrow \hat{U}_{k+1}, V \leftarrow \hat{V}_{k+1}, W \leftarrow \hat{W}_{k+1}, \vartheta \leftarrow \hat{\vartheta}$

Return U,V,W,ϑ

is the first-order equation grey system prediction model with one variable, which is abbreviated as the GM (1,1) model [22]. The estimation of its parameters is

$$\begin{pmatrix} a \\ b \end{pmatrix} = (B^T B)^{-1} B^T Y$$

where

$$B = \begin{pmatrix} -z^{(1)}(2) & 1 \\ -z^{(1)}(3) & 1 \\ \vdots & \vdots \\ -z^{(1)}(n) & 1 \end{pmatrix}, Y = \begin{pmatrix} x^{(0)}(2) \\ x^{(0)}(3) \\ \vdots \\ x^{(0)}(n) \end{pmatrix},$$

The time response equation of the mean GM (1,1) model is

$$\hat{x}^{(1)}(k) = (x^{(0)}(1) - \frac{b}{a})e^{-a(k-1)} + \frac{b}{a}, k = 1, 2, \ldots, n$$

3.3. Establishing the tensor ALS grey prediction model

To further explore the regularity and correlation of high-dimensional tensor data, which are large-scale data that are cumulative and complex, a tensor ALS GM (1,1) model is proposed, which is specifically defined as follows.

Definition 3.2. Let the high-dimensional tensor be χ. Then, the Tucker tensor decomposition model for solving χ is obtained by using the ALS method. First, the factor matrix is decomposed to simultaneously simulate the GM (1,1) model and update the initial factor matrix. Then, the updated factor matrix is combined with the core tensor and reduced to approximate the tensor. The GM (1,1) prediction model for time series using approximate tensors is called the tensor ALS GM (1,1) model (TALSGM (1,1) model).

The specific operation steps for the tensor ALS GM (1,1) model are as follows.

Step 1. The high-dimensional tensor data called the initial tensor are established using the original data.

Step 2. The Tucker tensor decomposition of the initial tensor is conducted. The factor matrix and the core tensor are obtained by the ALS algorithm. The factor matrix is simulated by the GM (1,1).

Step 3. By combining the factor matrix and the core tensor after the simulation, the approximate tensor is obtained according to the tensor time matrix (ttm) function in the tensor tool.

Step 4. The original time series for the initial tensor that is to be predicted and the corresponding time period are determined. The approximate tensor that is obtained in the third step is used, and the time series of the same time period for the approximate tensor are predicted by the GM (1,1) model.

Step 5. The tensor ALS GM (1,1) is used to calculate the simulated and predicted values, and the error analysis with the actual values is carried out to calculate the relative error and MAPE.

4. Numerical examples and experimental results

In this section, the correlations between week and week, day and day, hour and hour are first analysed, and then the validity of the tensor ALS grey model is analysed using three examples.

4.1. Relevance analysis of traffic data

This section mainly analyses the multi-modal form of the traffic flow tensor and studies the correlation of traffic flow. At

the same time, the concept of covariance correlation is used to analyse the correlation of traffic flow.

Data from the Institute of Urban Transportation, School of Transportation Engineering, Central South University [53] were collected from four direct lanes of Shaoshan Road, Changsha City, China, in the direction from south to north. The traffic flow is counted every minute. From September 17 to November 18, 2013, there were 63 days of traffic flow. The collector worked 24 h a day to collect 288 data points every five minutes.

Definition 4.1. Covariance: If $E[X - E(X)][Y - E(Y)]$ exists, it is called the covariance of random variables X and Y, which is denoted as $\mathrm{cov}(X, Y)$. That is,

$$\mathrm{cov}(X, Y) = E[X - E(X)][Y - E(Y)]$$

For discrete random vectors, the following equation can be obtained:

$$\mathrm{cov}(X, Y) = \sum_i \sum_j [x_i - E(X)][y_j - E(Y)]p_{ij}$$

where $P\{X = x_i, Y = y_j\} = p_{ij}$ and $i, j = 1, 2, 3, \ldots$ for continuous random variables. Then, the following equation can be obtained:

$$\mathrm{cov}(X, Y) = \int_{-\infty}^{\infty} \int_{-\infty}^{\infty} [x - E(X)][y - E(Y)]f(x, y)dxdy$$

Definition 4.2. Coefficient of correlation: The covariance is a "normalized" covariance, and its range varies between -1 and 1. The definition is

$$\rho_{XY} = \frac{\mathrm{cov}(X, Y)}{\sqrt{D(X)}\sqrt{D(Y)}}$$

Definition 4.3. Correlation coefficient matrix: In statistics and probability theory, the correlation coefficient matrix is the correlation coefficient between random variables corresponding to rows and columns. Assume a sequence of n free variables:

$$X = (x_1, x_2, \ldots, x_n)$$

Then, the correlation coefficient matrix is expressed as follows:

$$\varphi(X) = \begin{bmatrix} \rho_{11} & \rho_{12} & \cdots & \rho_{1n} \\ \rho_{21} & \rho_{22} & \cdots & \rho_{2n} \\ \cdots & \cdots & \cdots & \cdots \\ \rho_{n1} & \rho_{n2} & \cdots & \rho_{nn} \end{bmatrix}, \text{ where } \rho_{ij} = \rho_{x_i x_j}$$

According to the above definition, a correlation analysis between weeks and days or between hours and minutes will be carried out. Next, the correlation coefficient matrix of the traffic flow from the first week to the ninth week will be determined, as shown in Table 2.

Table 2 shows that the diagonal is 1, and the correlation coefficient is the same random variable. All the data in the correlation coefficient matrix are above 0.8, and the values near the diagonal are mostly approximately 0.9. The corresponding weekdays of the same week are more relevant, and the data associations that are longer than the time are not very large.

The following is a selection of the traffic flow data from Monday to Sunday for the second week. The specific correlation matrix is shown in Table 3.

Table 3 shows that the correlation between Monday and Friday is strong, and it is close to 0.9 or even higher than 0.9. Because people's attendance times are more balanced during working days than weekend days, such as students going to school and employees going to work, their time is relatively fixed, so they have strong correlations. Meanwhile, the correlation coefficient between Saturday and Sunday is only 0.82. On the weekend, the great uncertainty of time schedules is an important disturbance factor.

The following is the correlation between hours and the traffic flow. The traffic flow data from different time periods from 6 a.m. to 5 p.m. on Tuesday in the second week are selected. The correlation matrix is shown in Table 4.

As seen from Table 4, there is not much regularity in the data distribution, and the correlation between different time periods is not very large. According to the traffic flow data that are used by the above correlation coefficient matrix, the correlation between weeks, days, and hours can be further seen according to Figs. 3, 4, and 5.

Figs. 3 and 4 clearly show that the trends of the daytime traffic flows are very similar, and the data on the daytime traffic flow are highly correlated. Fig. 5 shows the different discontinuous traffic flow trend charts from 6 am to 5 p.m. on Tuesday of the second week, and the change in the traffic flow in an hour is overwhelming. The data are chaotic with a low degree of correlation.

4.2. Three numerical examples for the tensor ALS GM (1,1) model

In this section, to test the performance of the TALSGM (1,1) model, the simulation and prediction error analysis for three cases of short-term traffic flows [50] are analysed, and the simulation and prediction errors of the TALSGM (1,1) model are also analysed; then, these errors are calculated and compared with those of other grey prediction models, ANN and ARIMA. Meanwhile, the effects of approximate tensor data modelling and direct traffic flow data modelling are discussed.

Case 1. This section chooses the traffic flow data from the first week from Monday, 23 September to Sunday, 29 September. The empirical analysis of the tensor ALS GM (1,1) model predicts the traffic flow data for the first week from 10:30 to 10:45 a.m. on Thursday, 26 September. The operating steps for the tensor ALS GM (1,1) model are as follows.

Step 1. Construction of the initial tensor

The direction of the initial tensor dimension is divided into minutes, hours, and days, and the tensor is expressed as $\chi^{6\times8\times7}$. The minute direction of the initial tensor dimension is separated into six five-minute traffic flows from 10:00–10:30 a.m. and eight hourly traffic flows from 8 a.m. to 3 p.m. The day direction of the initial tensor dimension is from Monday to Sunday. The three dimensions together constitute the initial tensor. The traffic flow data for the initial tensor are calculated using MATLAB and shown in Fig. 6.

Step 2: Decompose the initial tensor using the Tucker tensor decomposition and analyse and process the factor matrix.

The initial tensor in Fig. 6 is decomposed by the Tucker tensor decomposition ALS algorithm. By analysing and processing the factor matrix in the decomposition result, an approximate tensor is obtained. The dimension of the core tensor is $\chi^{4\times1\times4}$, and the calculation results are shown in Fig. 7.

Fig. 7 shows the three-factor matrices and the core tensor that is decomposed by the initial tensor. Here, P1.core is the core tensor, the P1.core (:,:,1) matrix is represented as the first tangent plane of the core tensor, and other matrices are sequentially represented as the second, third, and fourth tangent planes. The meanings of the elements in Fig. 7 are explained below.

The element value of the first tangent plane matrix P1.core (:,:,1) of the core tensor is 2008.9, and its index is (1, 1, 1), which represents tensor T with rank 1 that is obtained by the tensor product of the first column of the factor matrix P1.U1, the first column of P1.U2 and the first column of P1.U3. The principal component of the tensor in the initial tensor is 2008.9, which is much larger than the values of the other elements in the core

Table 2
Matrix of the traffic flow coefficient for weekly Saturdays from week 1 to week 9.

	First	Second	Third	Fourth	Fifth	Sixth	Seventh	Eighth	Ninth
First	1.0000	0.8855	0.8811	0.8521	0.9078	0.8970	0.9217	0.9248	0.9033
Second	0.8855	1.0000	0.8453	0.8726	0.8835	0.8528	0.8862	0.8776	0.9124
Third	0.8811	0.8453	1.0000	0.8468	0.8367	0.8414	0.8592	0.8663	0.8502
Fourth	0.8521	0.8726	0.8468	1.0000	0.8690	0.8239	0.8333	0.8349	0.8897
Fifth	0.9078	0.8835	0.8367	0.8690	1.0000	0.9255	0.8645	0.8769	0.8808
Sixth	0.8970	0.8528	0.8414	0.8239	0.9255	1.0000	0.8941	0.9094	0.8295
Seventh	0.9217	0.8862	0.8592	0.8333	0.8645	0.8941	1.0000	0.9674	0.9013
Eighth	0.9248	0.8776	0.8663	0.8349	0.8769	0.9094	0.9674	1.0000	0.8843
Ninth	0.9033	0.9124	0.8502	0.8897	0.8808	0.8295	0.9013	0.8843	1.0000

Table 3
Incidence matrix of traffic flow data for seven days from Monday to Sunday in the second week.

	Monday	Tuesday	Wednesday	Thursday	Friday	Saturday	Sunday
Monday	1.0000	0.9155	0.9193	0.8881	0.9050	0.8485	0.8909
Tuesday	0.9155	1.0000	0.9008	0.8616	0.9119	0.8271	0.8803
Wednesday	0.9193	0.9008	1.0000	0.8503	0.8631	0.8410	0.8699
Thursday	0.8881	0.8616	0.8503	1.0000	0.8929	0.8868	0.8848
Friday	0.9051	0.9119	0.8631	0.8928	1.0000	0.8398	0.8593
Saturday	0.8485	0.8271	0.8410	0.8868	0.8398	1.0000	0.8277
Sunday	0.8909	0.8804	0.8699	0.8848	0.8593	0.8277	1.0000

Table 4
The correlation coefficient matrix of the traffic flow data in different time periods from 6 a.m. to 5 p.m. on Tuesday of the second week.

	6 a.m.	7 a.m.	8 a.m.	9 a.m.	10 a.m.	11 a.m.	12 p.m.	1 p.m.	2 p.m.
6 a.m.	1.00	0.68	0.20	0.16	−0.34	−0.42	0.31	0.01	0.02
7 a.m.	0.68	1.00	−0.05	−0.04	−0.10	−0.11	0.04	−0.01	0.14
8 a.m.	0.20	−0.05	1.00	−0.22	−0.43	−0.1	0.56	0.23	−0.65
9 a.m.	0.16	−0.04	−0.22	1.00	0.32	−0.50	0.01	0.08	0.76
10 a.m.	−0.34	−0.10	−0.43	0.32	1.00	0.05	−0.37	−0.18	0.69
11 a.m.	−0.42	−0.11	−0.12	−0.50	0.05	1.00	−0.14	−0.53	−0.38
12 p.m.	0.31	0.04	0.56	0.01	−0.37	−0.14	1.00	−0.34	−0.34
1 p.m.	0.01	−0.01	0.23	0.08	−0.18	−0.53	−0.34	1.00	−0.01
2 p.m.	0.02	0.14	−0.65	0.76	0.69	−0.38	−0.34	−0.01	1.00

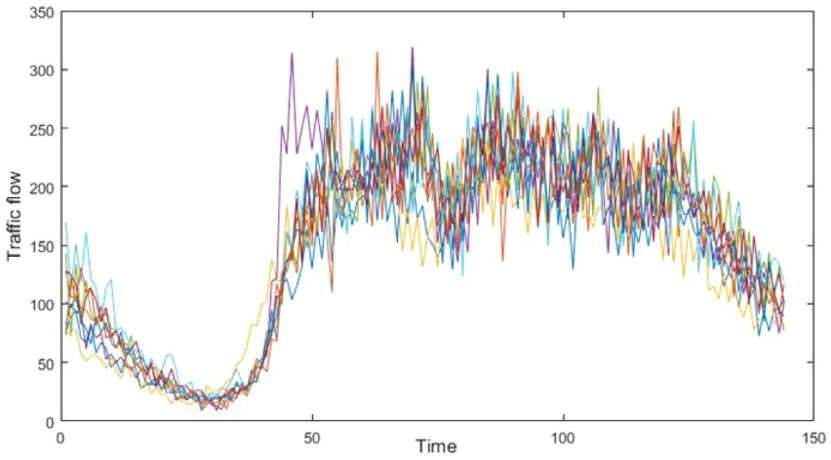

Fig. 3. Trend chart of the traffic flow from week 1 to week 9 on Saturdays.

tensor. The first column of factor matrix P1.U1 represents the main trend of the column fibres in the initial tensor, the first column of factor matrix P1.U2 represents the main trend of the row fibres and the first column of factor matrix P1.U3 represents the main trend of the tube fibres.

In the sub-factor matrix, P1.U2 represents the direction of time, which is the main trend of the traffic flow tensor of the initial tensor row. At this time, the simulation of P1.U2 by the GM (1,1) model is carried out. If the simulation effect is good enough, the simulation value is replaced by P1.U2. This step is performed to weaken the oscillation of the approximate tensor on the column fibres and improve the prediction effect of the tensor ALS GM (1,1) model.

If the dimension of the core tensor is changed from $\chi^{4\times1\times4}$ to $\chi^{4\times1\times4}$, then the factor matrix P1.U2 in the time direction becomes the matrix that is shown in Fig. 8. The second column of the factor matrix is an irregular column after the change, and the second column has a poor GM (1,1) simulation effect. Table 5 shows the simulation results and the average relative error maps for the first and second columns.

As shown in Table 4, the average relative error of the second column reaches 1.071469, which is very bad. At this time, the second column is regarded as a noise column, and we let the core

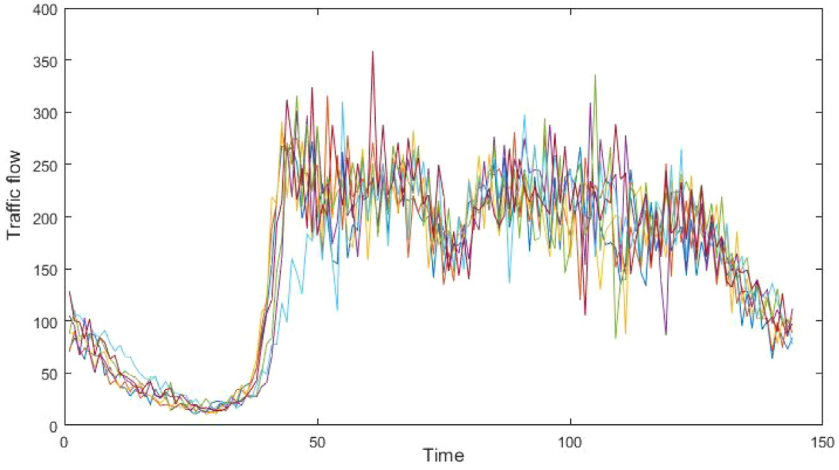

Fig. 4. Traffic flow trend chart for the seven days from Monday to Sunday in the second week.

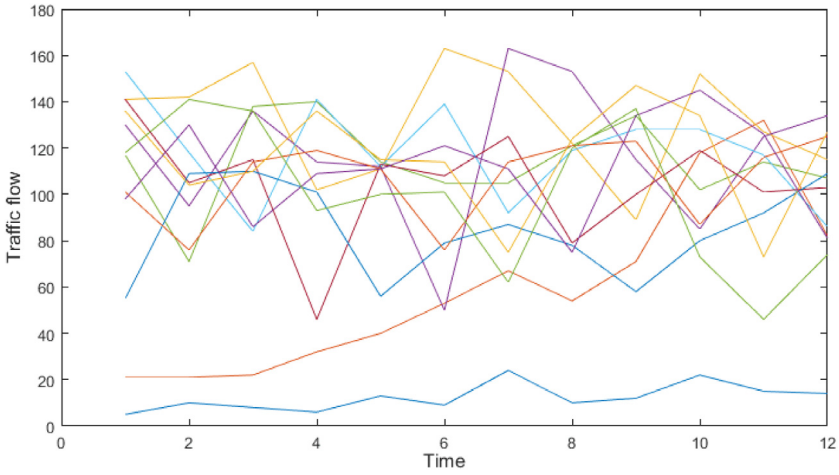

Fig. 5. Traffic flow trend charts for different periods of time from 6 a.m. to 5 p.m. on Tuesday of the second week.

Table 5
Simulation effects on the first and second columns of factor matrix P1.U2.

First column actual value of factor matrix	First column of simulation values	Second column actual value of factor matrix	The second column of simulation values
0.3545	0.3544	0.8326	0.8326
0.3577	0.355961	−0.2922	−0.08379
0.3823	0.354675	0.0864	−0.09113
0.3696	0.353395	−0.2758	−0.09912
0.3005	0.352118	0.1872	−0.1078
0.3108	0.350847	−0.0425	−0.11725
0.3691	0.349579	−0.2583	−0.12752
0.3748	0.348317	−0.1851	−0.13869
	MAPE = 0.062298		MAPE = 1.071469

tensor dimension be $\chi^{4\times1\times4}$, where MAPE is the mean absolute percentage error.

Step 3: Use the post-simulation factor matrix and core tensor to approximate the tensor

The approximate tensor is obtained by using the simulated factor matrix and the core tensor. At this time, the first column of the simulated P1.U1 matrix is combined with the other two factor matrices and the core tensor. The approximate tensor is calculated by the TTM function. The approximate tensor is shown in Fig. 9.

Step 4: Simulate and predict the TALSGM (1,1) model

Three traffic flow forecasting values in the 10:30–10:45 a.m. time interval on Thursday, 26 September are predicted. Six traffic flow data series in the 10:00–10:30 a.m. time interval on Thursday, 26 September are taken as the original time series using the approximate tensor.

The approximate tensor is:

$$X_1^{(0)} = (124.30,\ 106.45, 113.29, 103.10, 113.60, 109.29)$$

The original time series are accumulated once to obtain:

$$X_1^{(1)} = (124.30,\ 230.74,\ 344.05,\ 447.05,\ 560.65,\ 669.94)$$

The estimate parameters a and u are $(a, u) = (-0.0055,\ 106.936)$, so:

$$\hat{X}_1^{(1)}(k) = [x_1^{(0)}(1) + \frac{106.936}{0.0055}]e^{0.0055(k-1)} - \frac{106.936}{0.0055}$$

X2(:,:,1) =

114	152	126	112	51	100	125	119
158	107	111	108	91	74	127	126
90	69	89	133	93	111	80	117
109	91	103	82	101	103	106	50
70	110	121	101	73	128	128	112
162	82	119	117	73	87	128	126

X2(:,:,2) =

130	117	153	141	55	101	136	98
95	71	118	105	109	76	104	130
136	138	84	115	110	114	110	86
114	140	141	46	101	119	136	109
112	114	112	113	56	111	115	111
50	105	139	108	79	76	114	121

X2(:,:,3) =

108	67	149	135	116	66	81	125
71	167	83	124	93	113	128	116
98	94	64	80	103	105	83	90
120	87	128	107	70	131	99	118
123	138	134	141	92	82	171	134
52	32	98	142	93	126	49	131

X2(:,:,4) =

111	174	125	108	97	104	140	123
74	88	112	115	86	88	137	152
152	83	113	132	110	68	106	146
135	118	78	123	93	91	93	96
141	106	118	88	121	102	136	105
81	105	120	134	66	96	133	140

(a) The first four tangents of the initial tensor

X2(:,:,5) =

120	121	134	112	81	104	143	74
104	109	117	144	95	85	126	169
146	82	97	124	117	71	70	66
141	122	84	110	98	120	124	158
131	117	117	92	91	110	128	55
72	135	113	131	71	100	112	122

X2(:,:,6) =

55	174	117	123	74	87	138	156
121	136	110	121	117	62	117	142
94	80	74	113	126	111	94	114
117	124	141	64	119	123	124	107
80	120	121	120	70	126	140	125
78	87	129	144	96	75	109	144

X2(:,:,7) =

262	87	188	83	92	89	81	138
62	124	170	127	88	91	121	88
88	131	135	131	162	97	80	90
94	126	85	144	88	43	111	124
93	68	149	123	119	104	83	127
118	131	139	111	101	105	118	101

(b) The last three tangents of the initial tensor

Fig. 6. Initial tensor.

P1 is a tensor of size 6 x 8 x 7
P1.core is a tensor of size 4 x 1 x 4
P1.core(:,:,1) =
1.0e+03 *
2.0089
0.0000
0.0000
0.0000
P1.core(:,:,2) =
-0.0007
99.1109
0.0234
-0.0146
P1.core(:,:,3) =
0.0004
0.0148
-62.8160
-0.1802
P1.core(:,:,4) =
0.0004
-0.0088
0.1714
-59.7425

P1.U{1} =

0.4358	-0.3294	0.1719	-0.0360
0.4149	0.2933	-0.5285	-0.2439
0.3836	-0.4993	0.4014	0.2293
0.4008	0.3911	-0.1114	0.7872
0.4151	0.5048	0.5396	-0.4536
0.3972	-0.3851	-0.4758	-0.2474

P1.U{2} =

0.3539
0.3580
0.3821
0.3690
0.3003
0.3110
0.3692
0.3757

P1.U{3} =

0.3656	-0.1940	0.3744	0.5954
0.3732	-0.1471	-0.3758	-0.5912
0.3645	0.7367	-0.4130	0.3062
0.3870	-0.3076	-0.3532	0.1142
0.3793	0.2436	0.6118	-0.4140
0.3851	0.1690	0.2130	-0.0892
0.3902	-0.4642	-0.0601	0.0990

Fig. 7. Initial tensor decomposition results.

Table 6
Metrics for evaluating the effectiveness of the models.

Name	Abbreviation	Formulation
Mean absolute percentage error	MAPE	$\frac{1}{n}\left(\sum_{i=1}^{n}\Delta(i)\right)\times 100\%$
Mean absolute error	MAE	$\frac{1}{n}\sum_{i=1}^{n}\lvert\Delta\rvert$
Mean squares error	MSE	$\frac{1}{n}\sum_{i=1}^{n}\Delta^2$
Theil U statistic 1	U1	$\frac{\sqrt{\frac{1}{n}\sum_{i=1}^{n}\Delta^2}}{\sqrt{\frac{1}{n}\sum_{i=1}^{n}[x^{(0)}(k)]^2}+\sqrt{\frac{1}{n}\sum_{i=1}^{n}[\hat{x}_1^{(0)}(k)]^2}}$
Theil U statistic 2	U2	$\frac{\left[\sum_{i=1}^{n}\Delta^2\right]^{1/2}}{\left[\sum_{i=1}^{n}[x^{(0)}(k)]^2\right]^{1/2}}$

```
P1.U{2} =
    0.3545    0.8325
    0.3577   -0.2926
    0.3823    0.0857
    0.3696   -0.2755
    0.3005    0.1884
    0.3108   -0.0435
    0.3691   -0.2587
    0.3748   -0.1839
```

Fig. 8. Factor matrix P1.U2 after dimension change.

Bring 1, 2, …, 9 into the above equation to obtain:

$$\hat{X}_1^{(1)}(k) = (124.3, 232.2, 340.7, 449.9, 559.6, 669.9, 780.9, 892.5, 1004.7)$$

Next, perform a cumulative reduction on $\hat{X}_1^{(1)}(k)$to obtain the model prediction sequence $\hat{X}_1^{(0)}$ as:

$$\hat{X}_1^{(0)} = (124.30, 107.92, 108.52, 109.13, 110.34, 110.95, 111.57, 112.19)$$

The first six sequence values are the simulation values of the TALSGM (1,1) model, and the last three sequence values are the prediction values.

Step 5. Calculate the average absolute percentage error between the predicted sequence value and the actual value.

According to traffic flow data, the sequence of the actual traffic flow values during 10:00–10:45 a.m. on Thursday, 26 September is as follows:

$$X^{(0)} = (125.00, 112.00, 113.00, 78.00, 118.00, 120.00, 128.00, 111.00, 107.00)$$

Step 6. The inspection index is calculated, and $\Delta = x^{(0)}(k) - \hat{x}_1^{(0)}(k)$ and $\bar{\Delta} = \frac{x^{(0)}(k)-\hat{x}_1^{(0)}(k)}{x^{(0)}(k)}\Delta(k) = \left|\frac{x^{(0)}(k)-\hat{x}_1^{(0)}(k)}{x^{(0)}(k)}\times 100\%\right|, k = 1, 2, \ldots, n$ are set. The definition of the evaluation index is shown in Table 6.

In Table 6, since the first simulation value of the grey prediction model does not change, $k = 2, \ldots, n$ and $\frac{1}{n}$ is changed to $\frac{1}{n-1}$.

Through the above steps, the simulated value and predicted value of the TALSGM (1,1) model in the time period of 10:00–10:45 a.m. on Thursday, 26 September are calculated. There are 9 data points in total. The first 6 data points are used for simulation, and the last 3 data points are used for prediction. The models used for model comparison are GM (1,1) [22], ENGM (1,1) [37], ONGM (1,1) [36], and Verhulst [29] as well as the artificial neural network (ANN) [52] and ARIMA model [17]. The comparison results are shown in Table 7, and the results of the test indicators are shown in Table 8. In Table 7, only TALSGM (1,1) uses approximate tensor data, and the other four grey models are directly modelled with the original traffic flow data. ANN selects 5 groups of data before 10:45 a.m. for a total of 45 data points. The proportion of data groups set for training, verification and testing is 2:2:1. Due to the strong randomness of the model, Table 7 shows the best results. The ARIMA model selects 24 data points before 10:45 a.m. as training data, and the results are shown in Table 7.

Table 7 shows the simulation and prediction values and relative errors of each model. To further compare the effectiveness of each model, Fig. 10 is used to visually represent the relative error. As shown in Fig. 10, the first simulation value of the grey prediction model is constant, so only ANN and ARIMA have errors when k = 1. In addition to the fourth data, the simulation error of the TALSGM (1,1) model is the lowest, and the relative error of the three predicted values is also relatively low. Table 8 shows that in the comparison of the five grey models, the five inspection indexes of TALSGM (1,1) are better than those of GM (1,1), ENGM (1,1), ONGM (1,1) and the Verhulst model, with the exception that the U1 value of GM (1,1) is the same as that of TALSGM (1,1). Compared with ARIMA and ANN, in the simulation stage, the MAPE value of the TALSGM (1,1) model is the lowest, and the other four test indexes are slightly inferior to the best ARIMA model, but in the prediction stage, the five inspection indexes of TALSGM (1,1) are the best. To compare the inspection indexes more clearly, comparison charts of the MAPE and MAE results are shown in Figs. 11 and 12.

Case 2. The data are from Section 4.1. Twelve raw traffic flow data sets from Tuesday of the first week are selected, 24 September from 9:00 to 10:00 a.m., as shown in Table 6. The sample data are divided into two parts: the 6 data flows in the first part (9:00–9:30 a.m.) are used as the modelling data, and the second part (9:30–10:00 a.m.) is used as the test data for the model. The approximate tensor data are obtained from the steps in Section 3.3, and the process from case 1 is used for the first six data flows, which are given in Table 9.

H(:,:,1) =

113.8523	114.4061	114.0325	113.6602	113.2890	112.9191	112.5503	112.1828
112.0898	112.6351	112.2672	111.9006	111.5352	111.1710	110.8080	110.4462
96.6339	97.1040	96.7869	96.4708	96.1558	95.8418	95.5289	95.2169
92.5197	92.9697	92.6661	92.3635	92.0619	91.7613	91.4617	91.1630
105.2607	105.7727	105.4274	105.0831	104.7399	104.3979	104.0570	103.7172
111.5591	112.1018	111.7357	111.3709	111.0072	110.6447	110.2834	109.9233

H(:,:,2) =

117.6397	118.2120	117.8260	117.4412	117.0577	116.6755	116.2945	115.9147
99.8734	100.3592	100.0315	99.7049	99.3793	99.0548	98.7313	98.4089
110.3070	110.8436	110.4816	110.1209	109.7613	109.4028	109.0456	108.6895
112.8094	113.3582	112.9880	112.6191	112.2513	111.8848	111.5194	111.1552
105.7489	106.2633	105.9163	105.5704	105.2257	104.8821	104.5396	104.1982
99.1538	99.6361	99.3108	98.9865	98.6633	98.3411	98.0199	97.6999

H(:,:,3) =

105.8836	106.3987	106.0513	105.7050	105.3598	105.0157	104.6728	104.3310
111.1215	111.6620	111.2974	110.9340	110.5717	110.2106	109.8508	109.4920
88.7385	89.1702	88.8790	88.5888	88.2995	88.0112	87.7238	87.4373
107.7436	108.2677	107.9141	107.5618	107.2105	106.8604	106.5115	106.1637
126.7104	127.3268	126.9110	126.4966	126.0835	125.6718	125.2614	124.8524
90.1740	90.6126	90.3167	90.0218	89.7278	89.4348	89.1428	88.8517

H(:,:,4) =

124.1125	124.7162	124.3090	123.9030	123.4984	123.0951	122.6932	122.2925
106.2779	106.7949	106.4461	106.0985	105.7521	105.4067	105.0625	104.7195
113.1184	113.6686	113.2975	112.9275	112.5587	112.1912	111.8248	111.4597
102.9387	103.4395	103.1017	102.7650	102.4295	102.0950	101.7616	101.4293
113.4186	113.9703	113.5982	113.2272	112.8575	112.4890	112.1216	111.7555
109.1187	109.6495	109.2915	108.9346	108.5788	108.2243	107.8709	107.5186

H(:,:,5) =

111.5828	112.1256	111.7594	111.3945	111.0307	110.6682	110.3068	109.9466
117.9624	118.5363	118.1492	117.7634	117.3788	116.9955	116.6135	116.2327
95.8397	96.3059	95.9914	95.6780	95.3655	95.0541	94.7437	94.4344
119.8176	120.4004	120.0072	119.6154	119.2248	118.8354	118.4474	118.0606
104.5301	105.0386	104.6956	104.3537	104.0129	103.6733	103.3347	102.9973
106.7259	107.2451	106.8949	106.5458	106.1979	105.8511	105.5055	105.1609

H(:,:,6) =

115.9416	116.5056	116.1251	115.7459	115.3680	114.9912	114.6157	114.2415
116.1021	116.6669	116.2859	115.9062	115.5277	115.1504	114.7744	114.3996
100.5575	101.0466	100.7167	100.3878	100.0600	99.7332	99.4076	99.0829
113.9713	114.5257	114.1517	113.7790	113.4074	113.0371	112.6680	112.3001
112.5227	113.0701	112.7009	112.3329	111.9660	111.6004	111.2360	110.8728
107.1132	107.6343	107.2828	106.9325	106.5833	106.2352	105.8883	105.5426

H(:,:,7) =

125.7215	126.3331	125.9206	125.5094	125.0995	124.6910	124.2839	123.8780
108.7909	109.3201	108.9631	108.6073	108.2526	107.8992	107.5468	107.1956
114.1762	114.7316	114.3570	113.9835	113.6113	113.2403	112.8706	112.5020
102.7281	103.2278	102.8907	102.5547	102.2199	101.8861	101.5534	101.2217
108.2678	108.7945	108.4392	108.0851	107.7321	107.3803	107.0297	106.6802
114.7955	115.3540	114.9773	114.6018	114.2276	113.8546	113.4828	113.1122

Fig. 9. Approximate tensor.

Here, the TALSGM (1,1) model uses the 6 data flows in Table 10 for the modelling, and the latter 6 data flows in Table 9 are used for the prediction. Using step 5 of case 1, the results in Table 11 and Fig. 13 are obtained. In addition, in Table 9, the other four grey prediction models are simulated using the first six data flows in Table 9, and the latter six data flows are used for the predictions.

Table 11 shows that the MAPE of the TALSGM (1,1) model in the simulation period is slightly worse than those of the Verhulst model and the ONGM (1,1) model, but it is nearly four percentage points lower than that of the GM (1,1) model, which indicates that the accuracy of the TALSGM (1,1) model can be improved from the perspective of the data. From the MAPE of the prediction, the effect of the TALSGM (1,1) model is much better than those of the

Table 7
Simulated and forecasted values and errors of the seven models in case 1.

Raw tensor data	Approximate tensor data	GM (1,1)		ENGM (1,1)		ONGM (1,1)		Verhulst		ARIMA		ANN		TALSGM (1,1)	
$x^{(0)}(k)$	$x_1^{(0)}(k)$	$\hat{x}_1^{(0)}(k)$	$\Delta(k)$	$\hat{x}_1^{(0)}(k)$	$\Delta(k)$	$\hat{x}_1^{(0)}(k)$	$\Delta(k)$	$\hat{x}_1^{(0)}(k)$	$\Delta(k)$	$\hat{x}_1^{(0)}(k)$	$\Delta(k)$	$\hat{x}_1^{(0)}(k)$	$\Delta(k)$	$\hat{x}_1^{(0)}(k)$	$\Delta(k)$
125.00	124.30	125.00	0.00	125.00	0.00	125.00	0.00	125.00	0.00	117.71	5.83	149.89	19.92	124.30	0.00
112.00	106.45	103.73	7.39	93.951	16.12	100.26	10.48	68.41	4.97	109.92	1.85	109.11	2.58	107.95	1.41
113.00	113.30	105.91	6.27	99.362	12.07	100.34	11.21	92.28	17.84	107.79	4.61	107.97	4.45	108.65	4.10
78.00	103.44	108.14	38.64	104.937	34.54	100.46	28.79	111.98	31.83	105.08	3.47	90.74	16.33	109.36	5.72
118.00	113.97	110.42	6.43	110.682	6.20	100.66	14.70	119.68	7.52	117.81	0.16	107.81	8.63	110.07	3.43
120.00	109.65	112.74	6.05	116.600	2.83	101.00	15.83	111.74	3.48	112.61	6.16	109.7	8.58	110.78	1.03
128.00		115.118	10.06	122.698	4.14	101.57	20.65	91.90	28.20	106.39	16.88	115.82	9.51	110.95	13.32
111.00		117.541	5.89	128.982	16.20	102.51	7.65	159.94	44.07	106.09	4.42	109.35	1.49	111.57	0.51
107.00		120.016	12.17	136.456	26.59	104.08	2.73	206.47	92.96	105.80	1.12	122.08	14.09	112.19	4.85

Table 8
Metrics of the seven models for simulation and prediction in validation case 1.

Simulation	GM (1,1)	ENGM (1,1)	ONGM (1,1)	Verhulst	ARIMA	ANN	TALSGM (1,1)
MAPE	12.955	14.351	16.201	21.826	8.889	10.08	**3.138**
MAE	10.057	11.557	13.867	18.038	**8.207**	11.007	9.602
MSE	189.541	217.079	244.038	592.516	**145.43**	170.9	194.53
U1	0.062	0.067	0.072	0.111	**0.054**	0.058	0.062
U2	0.123	0.132	0.139	0.217	**0.108**	0.117	0.125
Prediction	GM (1,1)	ENGM (1,1)	ONGM (1,1)	Verhulst	ARIMA	ANN	ENGM (1,1)
MAPE	9.374	15.645	10.344	55.082	7.477	8.37	**6.227**
MAE	10.813	17.580	12.613	61.503	9.24	9.637	**7.603**
MSE	126.049	406.373	259.717	4530.9	164.18	126.2	**105.99**
U1	0.048	0.082	0.074	0.244	0.058	0.049	**0.045**
U2	0.097	0.174	0.139	0.582	0.111	0.097	**0.089**

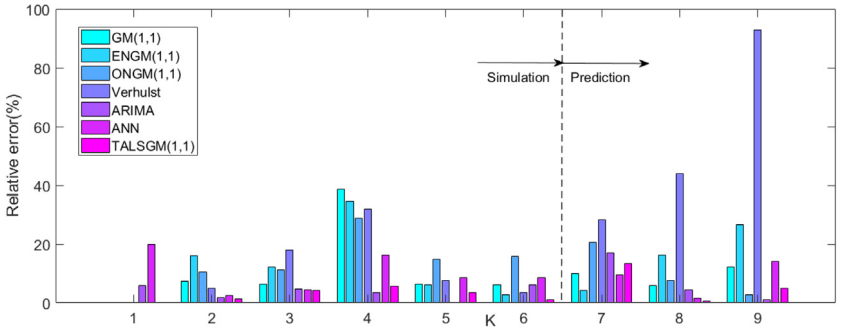

Fig. 10. Relative errors among the seven models for validation case 1.

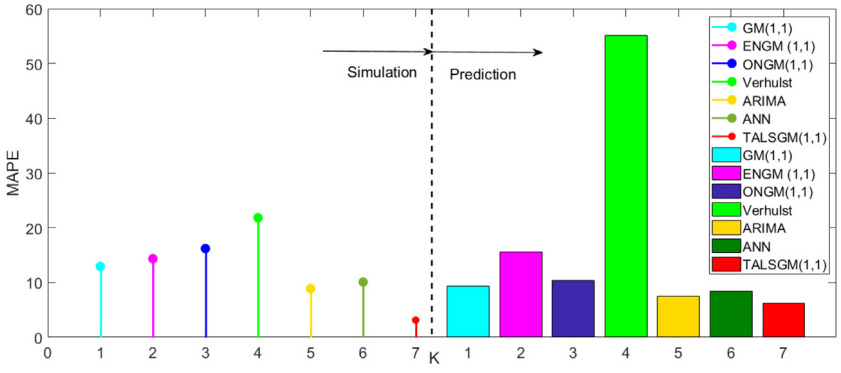

Fig. 11. MAPE among the seven models for validation case 1.

other four grey prediction models, and the prediction effect of the TALSGM (1,1) model using simulated tensor data is much better than that of the direct model using the original data. Fig. 13 shows that the prediction effect of the TALSGM (1,1) model is the best, and the simulation effect of the Verhulst model is equivalent to that of the ONGM (1,1) model. Overall, the effect of the TALSGM (1,1) model is better than that of the other four grey prediction models.

Case 3. Comparison of the initial tensor (GM (1,1) model) and approximate tensor data (TALSGM (1,1) model)

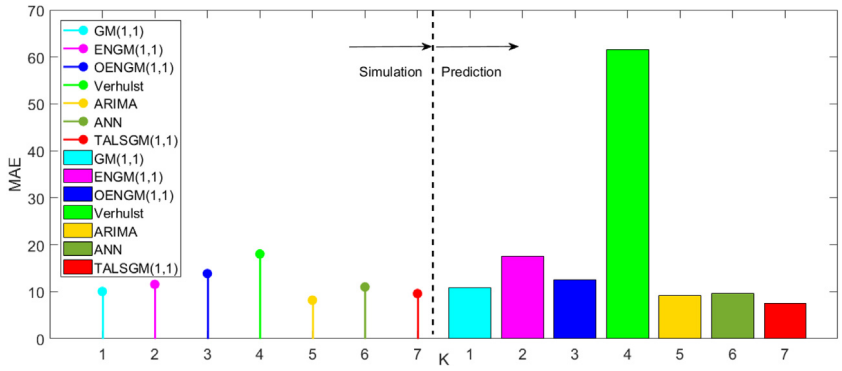

Fig. 12. MAE among the seven models for validation case 1.

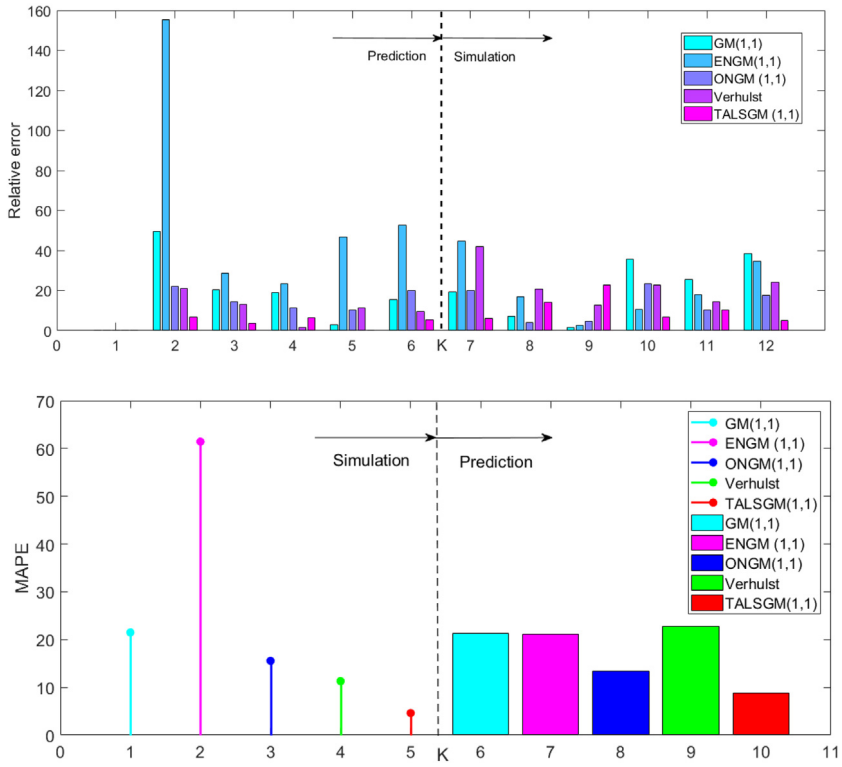

Fig. 13. Errors among the five models for case 2.

Table 9
The original data from 9:30 to 10:00 a.m. on 24 September.

Number	1	2	3	4	5	6	7	8	9	10	11	12
$X^{(0)}(k)$	117	71	138	140	114	105	105	121	132	102	114,	107

Table 10
Approximate tensor data from 9:30 to 10:00 a.m. on 24 September.

Number	1	2	3	4	5	6
$X_1^{(0)}(k)$	118.20	100.33	110.82	113.33	106.24	99.64

In this section, the initial tensors $X_2(:,:,1)$ to $X_2(:,:,6)$, which are the five-minute data in Fig. 6, are selected as the simulated data for 8:00–8:30 a.m. on Monday, and the GM (1,1) model is used. The first row of data from six consecutive sections of approximate tensors $H(:,:,1)$ to $H(:,:,6)$ in Fig. 9 is selected, which corresponds to the approximate tensor data from 8:00–8:30 a.m. for six consecutive weeks. The TALSGM (1,1) model is used to simulate the data, the comparison results are given in Table 12, and the error MAPE comparison results are given in Fig. 14.

Table 12 shows that the simulation effect of the GM (1,1) model with the initial tensor data is not good. The best simulation result occurs in the 6th week and is 8.891%. This result further shows that the 5-min traffic flow data are chaotic [54]. The GM (1,1) model with the original data is not ideal for 5-min traffic flow data. The TALSGM (1,1) model is used to avoid this chaotic phenomenon from approximate tensor data. The simulation result is only 11.839% in the third week and is less than 7% in the other five weeks, and the best simulation result is 3.166%. This result is nearly 10 times lower than that obtained when raw data are directly used, and the results of the other five weeks also show multiple declines. From the simulation error results of Fig. 14, it is clear that the six TALSGM (1,1) models have much lower errors than the GM (1,1) models. Thus, it is feasible to use the tensor model to represent traffic flow data, and the effect of the approximate tensor data is better than that from the direct

Table 11
Simulated and forecasted values and errors of the five models for case 2.

Number	Raw tensor data	Approximate tensor data	GM (1,1)		ENGM (1,1)		ONGM (1,1)		Verhulst		TALSGM (1,1)	
	$x^{(0)}(k)$	$x_1^{(0)}(k)$	$\hat{x}_1^{(0)}(k)$	$\Delta(k)$ (%)	$\hat{x}_1^{(0)}(k)$	$\Delta(k)$ (%)	$\hat{x}_1^{(0)}(k)$	$\Delta(k)$(%)	$\hat{x}_1^{(0)}(k)$	$\Delta(k)$(%)	$\hat{x}_1^{(0)}(k)$	$\Delta(k)$ (%)
$k=1$	117.00	118.21	117.00	0.00	117.00	0.00	117.00	0.00	117.00	0.00	118.21	0.00
$k=2$	71.00	100.36	106.22	49.60	181.38	155.47	86.80	22.25	85.87	20.95	107.25	6.87
$k=3$	138.00	110.84	109.80	20.43	177.6	28.69	118.20	14.34	119.87	13.13	106.67	3.76
$k=4$	140.00	113.36	113.51	18.82	172.96	23.54	124.37	11.16	137.68	1.66	106.09	6.41
$k=5$	114.00	106.26	117.34	2.93	167.27	46.73	125.58	10.16	126.76	11.20	105.51	0.07
$k=6$	105.00	99.64	121.30	15.52	160.31	52.68	125.82	19.83	95.06	9.47	104.94	5.32
MAPE				21.482		61.422		15.548		11.281		**4.613**
Prediction												
$k=7$	105.00		125.39	19.42	151.77	44.55	125.86	19.87	60.88	42.02	104.36	06.10
$k=8$	121.00		129.62	7.13	141.31	16.79	125.87	4.03	96.02	20.64	103.80	14.21
$k=9$	132.00		143.00	1.51	128.49	2.66	125.87	4.64	115.11	12.80	103.24	22.95
$k=10$	102.00		138.52	35.8	112.78	10.57	125.87	23.41	125.13	22.67	102.69	6.70
$k=11$	114.00		143.20	25.61	93.53	17.96	125.87	10.42	130.29	14.29	102.13	10.41
$k=12$	107.00		148.03	38.34	69.93	34.64	125.87	17.64	132.93	24.24	101.58	5.06
MAPE				21.304		21.193		13.333		22.777		**8.795**

Table 12
Comparison of the results from using the initial tensor data and approximate tensor data.

Raw tensor data	Approximate tensor data	GM (1,1)	TALSGM (1,1)	Raw tensor data	Approximate tensor data	GM (1,1)	TALSGM (1,1)
114	113.85	114.00	113.85	130	117.64	130.00	117.64
158	112.09	120.84	102.01	95	99.87	121.54	106.73
90	96.63	119.30	102.81	136	110.31	110.65	106.15
109	92.52	117.77	103.61	114	112.81	100.74	105.58
70	105.26	116.27	104.41	112	105.75	91.72	105.00
162	111.56	114.78	105.22	50	99.15	83.50	104.43
MAPE (%)		**31.871**	**6.769**			**28.663**	**4.615**
108	105.88	108.00	105.88	111	124.11	111.00	124.11
71	111.12	94.90	105.66	74	106.28	116.11	107.78
98	88.74	93.84	105.28	152	113.11	116.36	108.38
120	107.74	92.79	104.90	135	102.94	116.60	108.97
123	126.71	91.76	104.52	141	113.42	116.84	109.57
52	90.17	90.74	104.14	81	109.12	117.09	110.17
MAPE		**32.093**	**11.839**			**31.135**	**3.166**
120	111.58	120.00	111.58	55	115.94	55	115.94
104	117.96	132.59	111.77	121	116.10	118.61	111.26
146	95.84	125.36	110.35	94	100.56	107.25	110.66
141	119.81	118.52	108.96	117	113.97	96.98	110.05
131	104.53	112.06	107.57	80	112.52	87.69	109.45
72	106.73	105.94	106.21	78	107.11	79.29	108.85
MAPE		**28.835**	**6.571**			**8.891**	**4.400**

use of the original tensor data. This result shows that the tensor ALS method is a feasible scheme to establish a grey prediction model.

4.3. Analysis of the results

The case is mainly analysed from two perspectives. First, the traffic data correlations at the weekly, daily and minute scales are analysed, and it is found that the time correlation of the circumferential pattern in the tensor model is the largest. Tensor deep mining and analysis of the internal correlations of traffic data can improve the reconstruction accuracy and reconstruction ability of traffic data. Therefore, the tensor models of case 1 and case 2 based on the tensor representation of traffic flow data are established, and these models make full use of the correlation of the circumferential model. The results indicate that it is feasible to study traffic flow data using the tensor ALS method, and the approximate tensor data that are obtained are also feasible.

Second, case 1 and case 2 also show that the effect of the TALSGM (1,1) model is better than that of the GM (1,1) model. When directly applied to the original traffic flow data, the simulation accuracy of the first experimental results decreased from 12.955% to 10.520%, and the prediction accuracy decreased from 9.374% to 6.227%. Meanwhile, the simulation and prediction accuracies of the second experimental results are also obviously improved, especially the prediction accuracy, which decreased from 21.304% to 8.795%. Meanwhile, the comparison between the TALSGM (1,1) model and other grey prediction models, namely, the GM (1,1), ENGM (1,1), ONGM (1,1) and Verhulst models, is reflected in two traffic flow examples. Case 3 shows that the data modelling of the approximate tensor is more effective than that of direct traffic flow data modelling, and the specific comparison results are given in Table 8 and Fig. 12.

5. Conclusion

In this paper, the high-dimensional tensor is used to represent multi-mode traffic flow data. The core tensor and factor matrix are obtained by using the Tucker tensor decomposition ALS algorithm, which fully reflects the overall trend of the traffic flow data. The factor matrix is tested by using the grey prediction model GM (1,1), and the tensor time matrix function is used to obtain the factor matrix, which establishes the grey prediction model. Based on the principle of the Tucker tensor decomposition least squares and the modelling mechanism of the grey prediction

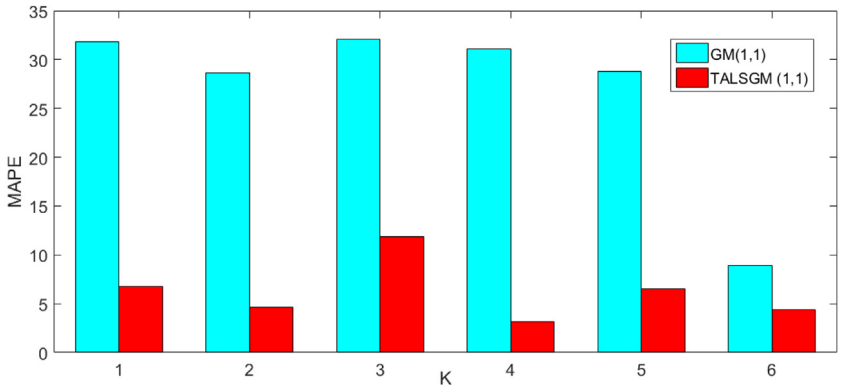

Fig. 14. Errors among the initial tensor data and approximate tensor data.

model, the tensor ALS grey model is proposed, and the algorithm and steps of the model are obtained.

Taking the short-term traffic flow prediction of Shaoshan Road in Changsha City, Hunan Province, as an example, the correlation analysis of the minute, day and week tensor models of the 63-day traffic flow data is carried out. According to the multi-mode characteristics of the data, a minute-day-week tensor grey prediction model (TALSGM (1,1) model) is established. Two different time periods of data are used for the case analysis, and the results of the analysis show that the simulation and prediction results of the TALSGM (1,1) model are basically better than those of the GM (1,1) model, ENGM (1,1) model and ONGM (1,1) model. Meanwhile, the approximate tensor data are used to verify the other three grey prediction models, and the effect is also better than directly using the original traffic flow data.

Declaration of competing interest

No author associated with this paper has disclosed any potential or pertinent conflicts which may be perceived to have impending conflict with this work. For full disclosure statements refer to https://doi.org/10.1016/j.asoc.2020.106145.

CRediT authorship contribution statement

Huiming Duan: Conceptualization, Methodology, Formal analysis, Writing - original draft, Writing - review & editing. **Xinping Xiao:** Methodology, Funding acquisition, Project administration, Supervision. **Jie Long:** Investigation, Software, Visualization. **Yongzhi Liu:** Validation, Data curation.

Acknowledgments

The authors are grateful to the editor for their valuable comments. This work is supported by the National Natural Science Foundation of China (71871174); Project of Humanities and Social Sciences Planning Fund of Ministry of Education of China (18YJA630022).

References

[1] M. Jonathan, F.R. John, Z. Rocco, An evaluation of HTM and LSTM for short-term arterial traffic flow prediction, IEEE Trans. Intell. Transp. Syst. 1 (8) (2018) 1–11, http://dx.doi.org/10.1109/TITS.2018.2843349.

[2] C. Chen, Y. Wang, L. Li, et al., The retrieval of intra-day trend and its influence on traffic prediction, Transp. Res. C 22 (2012) 103–118, http://dx.doi.org/10.1016/j.trc.2011.12.006.

[3] R. Herman, Technology human interaction and complexity: reflections on vehicular traffic science, Oper. Res. 40 (2) (1992) 199–212, http://dx.doi.org/10.1287/opre.40.2.199.

[4] D.H. Wang, Theory of Traffic Flow, China Communications Press, Beijing, 2002.

[5] V.J. Stephanesdes, G. Panos, R.A. Plum, Improved estimation of traffic flow for Real-Time control (Discussion and closure), Transp. Res. Rec. (1981) 28–37.

[6] M.H. Hamed, H.R. Al-Masaeid, Z.M. Bani, Short-term prediction of traffic volume in urban arterials, J. Transp. Eng. 121 (3) (1995) 249–254.

[7] M. Castro-Neto, Y.S. Jeong, M.K. Jeong, et al., Online-SVR for short-term traffic flow prediction under typical and atypical traffic conditions, Expert Syst. Appl. 36 (3) (2009) 6164–6173, http://dx.doi.org/10.1016/j.eswa.2008.07.069.

[8] A. Aussem, J. Campbell, F. Murtagh, Wavelet based feature extraction and decomposition strategies for financial forecasting, J. Comput. Intell. Finance 6 (2) (1998) 5212.

[9] T.T. Tchrakian, B. Basu, M. Mahony, Real-time traffic flow forecasting using spectral analysis, IEEE Trans. Intell. Transp. Syst. 13 (2) (2012) 519–526, http://dx.doi.org/10.1109/TITS.2011.2174634.

[10] A.Y. Cheng, X. Jiang, Y.F. Li, Muliple sources and multiple measures based traffic flow prediction using the chaos theory and support vector regression method, Physica A 466 (2017) 422–434, http://dx.doi.org/10.1016/j.physa.2016.09.041.

[11] J.Q. Wang, I. Tsapakis, C. Zhong, A space–time delay neural network model for travel time prediction, Eng. Appl. Artif. Intell. 52 (2016) 145–160, http://dx.doi.org/10.1016/j.engappai.2016.02.012.

[12] W.L. Min, L. Wynter, Real-time road traffic prediction with spatio-temporal correlations, Transp. Res. C 19 (4) (2011) 606–616, http://dx.doi.org/10.1016/j.trc.2010.10.002.

[13] S.F. Cheng, F. Lu, P. Peng, et al., Short-term traffic forecasting: An adaptive ST-KNN model that considers spatial heterogeneity, Comput. Environ. Urban Syst. 71 (9) (2018) 186–198, http://dx.doi.org/10.1016/j.compenvurbsys.2018.05.009.

[14] J. Guo, W. Huang, B.M. Williams, Adaptive Kalman filter approach for stochastic traffic flow rate prediction and uncertainty quantification, Transp. Res. C 43 (1) (2014) 50–64, http://dx.doi.org/10.1016/j.trc.2014.02.006.

[15] Y.R. Zhang, Y.L. Zhang, A. Haghani, A hybrid short-term traffic flow forecasting method based on spectral analysis and statistical volatility model, Transp. Res. C 43 (1) (2014) 65–78, http://dx.doi.org/10.1016/j.trc.2013.11.011.

[16] W.C. Hong, Traffic flow forecasting by seasonal SVR with chaotic simulated annealing algorithm, Neurocomputing 74 (12) (2011) 2096–2107, http://dx.doi.org/10.1016/j.neucom.2010.12.032.

[17] J.W. Yang, X.P. Xiao, S.H. Mao, Grey coupled prediction model for traffic flow panel data characteristics, Entropy 18 (12) (2016) 454–464, http://dx.doi.org/10.3390/e18120454.

[18] H. Tan, G.D. Feng, J. Feng, et al., A tensor-based method for missing traffic data completion, Transp. Res. C 28 (2013) 15–27, http://dx.doi.org/10.1016/j.trc.2012.12.007.

[19] H.C. Tan, Y.K. Wu, G.D. Feng, et al., A new traffic prediction method based on dynamic tensor, Proc. Soc. Behav. Sci. 96 (2013) 2431–2442, http://dx.doi.org/10.1016/j.sbspro.2013.08.272.

[20] H.M. Duan, X.P. Xiao, A multimode dynamic short-term traffic flow grey prediction model of high-dimension tensors, Complexity (2019) http://dx.doi.org/10.1155/2019/9162163.

[21] H.M. Duan, Y.Z. Liu, D. Wang, et al., Prediction of a multimode coupling model based on traffic flow tensor data, J. Intell. Fuzzy Syst. 36 (2) (2019) 1691–1703, http://dx.doi.org/10.3233/JIFS-18804.

[22] J.L. Deng, Estimate and Decision of Grey System, Huazhong University of Science and Technology Press, Wuhan, 2002.

[23] S.H. Mao, X.P. Xiao, M.Y. Gao, et al., Nonlinear fractional order grey model of urban traffic flow short term prediction, J. Grey Syst. 30 (4) (2018) 1–17.
[24] Z.X. Wang, P.Y. Yao, Grey relational analysis of economic policy uncertainty in selected European union countries, Econ. Comput. Econ. Cybern. Stud. Res. 52 (2) (2018) 251–265, http://dx.doi.org/10.24818/18423264/52.2.18.15.
[25] B. Zeng, H.M. Duan, Y.F. Zhou, A new multivariable grey prediction model with structure compatibility, Appl. Math. Model. (75) (2019) 385–397, http://dx.doi.org/10.1016/j.apm.2019.05.044.
[26] M. Xie, L.F. Wu, B. Li, et al., A novel hybrid multivariate nonlinear grey model for forecasting the traffic-related emissions, Appl. Math. Model. 77 (2020) 1242–1254, http://dx.doi.org/10.1016/j.apm.2019.09.013.
[27] B. Zeng, C. Li, Forecasting the natural gas demand in China using a self-adapting intelligent grey model, Energy (112) (2016) 810–825, http://dx.doi.org/10.1016/j.energy.2016.06.090.
[28] H.M. Duan, G.Y. Lei, K.L. Shao, Forecasting crude oil consumption in China using a grey prediction model with an optimal fractional-order accumulating operator, Complexity (2018) 1–12, http://dx.doi.org/10.1155/2018/3869619.
[29] S. Ding, Y.G. Dang, N. Xu, The optimization of grey Verhulst model and its application, J. Grey Syst. 27 (2015) 1–12.
[30] Z.X. Wang, Q. Li, Modelling the nonlinear relationship between CO2 emissions and economic growth using a PSO algorithm-based grey Verhulst model, J. Cleaner Prod. 207 (2019) 214–224, http://dx.doi.org/10.1016/j.jclepro.2018.10.010.
[31] L.F. Wu, S.F. Liu, Y.J. Yang, Grey double exponential smoothing model and its application on pig price forecasting in China, Appl. Soft Comput. 39 (2016) 117–123, http://dx.doi.org/10.1016/j.asoc.2015.09.054.
[32] B. Zeng, C. Li, Improved multi-variable grey forecasting model with a dynamic background value coefficient and its application, Comput. Ind. Eng. 118 (2018) 278–290, http://dx.doi.org/10.1016/j.cie.2018.02.042.
[33] N.M. Xie, S.F. Liu, Discrete grey forecasting model and its optimization, Appl. Math. Model. 33 (2009) 1173–1186, http://dx.doi.org/10.1016/j.apm.2008.01.011.
[34] N.M. Xie, S.F. Liu, Y.J. Yang, et al., On novel grey forecasting model based on non-homogeneous index sequence, Appl. Math. Model. 37 (7) (2013) 5059–5068, http://dx.doi.org/10.1016/j.apm.2012.10.037.
[35] L.F. Wu, S.F. Liu, W. Cui, et al., Non-homogenous discrete grey model with fractional-order accumulation, Neural Comput. Appl. 25 (2014) 1215–1221, http://dx.doi.org/10.1007/s00521-014-1605-1.
[36] P.Y. Chen, H.M. Yu, Foundation settlement prediction based on a novel NGM model, Math. Probl. Eng. (2014) 1–8, http://dx.doi.org/10.1155/2014/242809.
[37] X. Ma, Z. Liu, Predicting the cumulative oilfield production using the novel grey ENGM model, J. Comput. Theoret. Nanosci. 13 (1) (2016) 89–95, http://dx.doi.org/10.1166/jctn.2016.4773.
[38] X. Ma, W.Q. Wu, B. Zeng, et al., The conformable fractional grey system model, ISA Trans. (2019) 1–17, http://dx.doi.org/10.1016/j.isatra.2019.07.009.
[39] Z.X. Wang, D.D. Li, H.H. Zheng, Model comparison of GM(1, 1) and DGM(1, 1) based on Monte–Carlo simulation, Physica A (2019) http://dx.doi.org/10.1016/j.physa.2019.123341.
[40] W.Q. Wu, X. Ma, B. Zeng, et al., Forecasting short-term renewable energy consumption of China using a novel fractional nonlinear grey Bernoulli model, Renew. Energy 140 (2019) 70–87, http://dx.doi.org/10.1016/j.renene.2019.03.006.
[41] Y.G. Wang, Z. Chen, Z. Gao, M. Chen, A generalization of the GM(1, 1) direct modeling method with a step by step optimizing grey derivative's whiten values and its applications, Kybernetes 33 (2) (2004) 382–389, http://dx.doi.org/10.1108/03684920410514391.
[42] L.F. Wu, N. Li, Y.J. Yang, Prediction of air quality indicators for the Beijing-Tianjin-Hebei region, J. Cleaner Prod. 196 (2018) 682–687, http://dx.doi.org/10.1016/j.jclepro.2018.06.068.
[43] J. Xia, X. Ma, W.Q. Wu, et al., Application of a new information priority accumulated grey model with time power to predict short-term wind turbine capacity, J. Cleaner Prod. 244 (2020) 1–38, http://dx.doi.org/10.1016/j.jclepro.2019.118573.
[44] J. Ye, Y. Dang, B. Li, Grey–Markov prediction model based on background value optimization and central-point triangular whitenization weight function, Commun. Nonlinear Sci. Numer. Simul. 54 (2018) 320–330, http://dx.doi.org/10.1016/j.cnsns.2017.06.004.
[45] C.I. Chen, S.J. Huang, The necessary and sufficient condition for GM(1, 1) grey prediction model, Appl. Math. Comput. 219 (11) (2013) 6152–6162, http://dx.doi.org/10.1016/j.amc.2012.12.015.
[46] C.I. Hsu, Y.H. Wen, Forecasting Trans-Pacific Air Traffic by Grey Model, American Society of Civil Engineers-Task Committee Reports, 1999, pp. 103–110.
[47] H. Guo, X.P. Xiao, J. Forrest, Urban road short- term traffic flow forecasting based on the delay and nonlinear grey model, J. Transp. Syst. Eng. Inf. Technol. 13 (2013) 60–66, http://dx.doi.org/10.1016/S1570-6672(13)60129-4.
[48] A. Bezuglov, G. Comert, Short-term freeway traffic parameter prediction: Application of grey system theory models, Expert Syst. Appl. 62 (2016) 284–292, http://dx.doi.org/10.1016/j.eswa.2016.06.032.
[49] X.P. Xiao, J.W. Yang, S.H. Mao, An improved seasonal rolling grey forecasting model using a cycle truncation accumulated generating operation for traffic flow, Appl. Math. Model. 51 (2017) 386–404, http://dx.doi.org/10.1016/j.apm.2017.07.010.
[50] X.P. Xiao, H.M. Duan, A new grey model for traffic flow mechanics, Eng. Appl. Artif. Intell. (2020) http://dx.doi.org/10.1016/j.engappai.2019.103350.
[51] J. Lu, W.D. Xie, H.B. Zhou, et al., An optimized nonlinear grey Bernoulli model and its applications, Neurocomputing 177 (2016) 206–214, http://dx.doi.org/10.1016/j.neucom.2015.11.032.
[52] H.M. Duan, X.P. Xiao, Q.Z. Xiao, An inertia grey discrete model and its application in short-term traffic flow prediction and state determination, Neural Comput. Appl. (2019) 1–17, http://dx.doi.org/10.1007/s00521-019-04364-w.
[53] M. Li, Central south university openits data. http://www.openits.cn/openPaper/567.jhtml.
[54] Y. Li, X. Jiang, H. Zhu, et al., Multiple measures-based chaotic time series for traffic flow prediction based on Bayesian theory, Nonlinear Dynam. 85 (1) (2016) 179–194, http://dx.doi.org/10.1007/s11071-016-2677-5.